

Electronic Supplemental information  
for

**Statically and Dynamically Flexible Hydrogen-bonded Frameworks Based on  
4,5,9,10-Tetrakis(4-carboxyphenyl)pyrene**

Taito Hashimoto, Ryusei Oketani, Aasato Inoue, Kohei Okubo, Kouki Oka, Norimitsu Tohnai,  
Kazuhide Kamiya, Shuji Nakanishi and Ichiro Hisaki\*

**Contents**

1. General
2. Experimental data

**Table S1** Crystal data for **CP-Py-1(DCB)**, **CP-Py-1(TCB)**, **CP-Py-1(DMAni)**, **CP-Py-2(DCB)**,  
**CP-Py-2(TCB)**, **CP-Py-2(DMAni)**, **CP-Py-3** and **CP-Py-1(MeNaph)**

**Fig. S1** PXRD pattern of **CP-Py-2(DCB)** after added DCB.

**Fig. S2** TG-DTA curves of **CP-Py-1(DCB)**.

**Fig. S3** Morphology of a single crystal and the corresponding molecular arrangements of **CP-Py-1(DCB)**.

**Fig. S4** Visualized void surface of **CP-Py-3**

**Fig. S5** CO<sub>2</sub> (green circle) and N<sub>2</sub> (black triangle) sorption isotherms of **CP-Py-3** recorded at 195 K and 77 k, respectively.

**Fig. S6** BET plot of **CP-Py-3** based on CO<sub>2</sub> adsorption isotherm.

**Fig. S7** Anomalous absorption behavior of **CP-Py-3** in CO<sub>2</sub> adsorption experiments.

**Fig. S8** TG-DTA curves of **CP-Py-1(TCB)**.

**Fig. S9** <sup>1</sup>H NMR spectrum of **CP-Py-1(TCB)** dissolved in DMSO-*d*<sub>6</sub>.

**Fig. S10** TG-DTA curves of **CP-Py-1(DMAni)**.

**Fig. S11** <sup>1</sup>H NMR spectrum of **CP-Py-1(DMAni)** dissolved in DMSO-*d*<sub>6</sub>.

**Fig. S12** PXRD pattern changes from **CP-Py-1(TCB)** to **CP-Py-2(TCB)**.

**Fig. S13** PXRD pattern changes from **CP-Py-1(DMAni)** to **CP-Py-2(DMAni)**.

**Fig. S14** PXRD pattern of **CP-Py-2(TCB)** after added TCB.

**Fig. S15** PXRD pattern of **CP-Py-2(DMAni)** after added DMAni.

**Fig. S16** Structural similarity of **CP-Py-1(TCB)** and **CP-Py-1(DMAni)**.

**Fig. S17** Definition of the structural parameters:  $\omega_{(\text{torsion})}$ ,  $\omega_{(\text{twist})}$ , and  $\omega_{(\text{bent})}$ .

**Fig. S18** Selected side views of the H-bonded dimer moieties of **CP-Py-1(DCB)**, **CP-Py-2(DCB)**,  
**CP-Py-1(TCB)**, **CP-Py-2(TCB)**, **CP-Py-1(DMAni)** and **CP-Py-2(DMAni)**.

3. References

## 1. General

All reagents and solvents were used as received from commercial suppliers.  $^1\text{H}$  and  $^{13}\text{C}$  NMR spectra were measured on a Bruker AV400M (400 MHz) spectrometer. Residual proton and carbon of deuterated solvents were used as internal standards for the measurements:  $\delta = 7.26$  ppm ( $\text{CDCl}_3$ ) and  $\delta = 2.50$  ppm ( $\text{DMSO}-d_6$ ) for  $^1\text{H}$  NMR,  $\delta = 77.16$  ppm ( $\text{CDCl}_3$ ) and  $\delta = 39.52$  ppm ( $\text{DMSO}-d_6$ ) for  $^{13}\text{C}$  NMR. HR-MS analyses were conducted on a JEOL JMS-700 instrument. Thermo gravimetric (TG) analyses were performed on Rigaku Thermo plus EVO2 (TG-DTA8122) under an  $\text{N}_2$  purge (300 mL/min) at a heating rate of  $5\text{ }^\circ\text{C min}^{-1}$ . Crystal structures were drawn using Mercury<sup>S1</sup> software. Powder X-ray diffraction (PXRD) data were collected on PANalytical XPert PRO X'Celetor (45 kV, 40 mA) using Cu-K $\alpha$  radiation at room temperature with a scan rate of  $1.2^\circ\text{min}^{-1}$  or on Rigaku MiniFlex 600 (40 kV, 15 mA) using Cu-K $\alpha$  radiation at room temperature with a scan rate of  $4^\circ\text{min}^{-1}$ .

**Single crystal X-ray or electron diffraction measurement and analysis.** **CP-Py-1(DCB), CP-Py-1(TCB), CP-Py-2(DCB), CP-Py-2(TCB)** and **CP-Py-1(MeNaph)** were collected at 113 K with a two-dimensional X-ray detector (PILATUS 200K/R) equipped on a Rigaku XtaLAB P200 diffractometer by using Mo-K $\alpha$  radiation monochromated with multilayer mirror ( $\lambda = 0.71073\text{ \AA}$ ). Diffraction data of **CP-Py-1(DMAri), CP-Py-2(DMAri)** and **CP-Py-3** was collected with a two-dimensional X-ray detector (Pilatus 100K) at SPring-8 (BL40XU) by using synchrotron radiation ( $\lambda = 0.81106\text{ \AA}$ ). Diffraction Data collection, cell refinement, and data reduction were carried out with CrysAlis PRO.<sup>S2</sup> SHELXT<sup>S3</sup> was used for the structure solution of the crystals. These calculations were performed with the observed reflections [ $I > 2\sigma(I)$ ] with the program OLEX-2 crystallographic software.<sup>S4</sup> Structural refinement was performed by SHELXL.<sup>S5</sup> All non-hydrogen atoms were refined with anisotropic displacement parameters, and hydrogen atoms were placed in idealized positions and refined as rigid atoms with the relative isotropic displacement parameters. For structural analysis of **CP-Py-1(TCB), CP-Py-1(DMAri)** and **CP-Py-3**, SQUEEZE function equipped in the PLATON program was used to treat severely disordered solvent molecules in voids.<sup>S6</sup>

**Gas sorption experiments.** The activated bulk sample of **CP-Py-3** was used for gas sorption measurements, which were performed on BELSORP-max (BEL, Japan) or Micromeritics 3Flex. The adsorption isotherms of  $\text{N}_2$ ,  $\text{CO}_2$  were corrected at 77K and 195 K, respectively. Brunauer–Emmett–Teller (BET) specific surface area:  $S_{\text{A(BET)}}$  was based on  $\text{CO}_2$  absorption isotherms.

## 2. Experimental data

**Table S1.** Crystal data for **CP-Py-1(DCB)**, **CP-Py-1(TCB)**, **CP-Py-1(DMA*n*)**, **CP-Py-2(DCB)**, **CP-Py-2(TCB)**, **CP-Py-2(DMA*n*)**, **CP-Py-3** and **CP-Py-1(MeNaph)**

	<b>CP-Py-1(DCB)</b>	<b>CP-Py-2(DCB)</b>	<b>CP-Py-3</b>
Formular	C <sub>44</sub> H <sub>26</sub> O <sub>8</sub> ·4(C <sub>6</sub> H <sub>4</sub> Cl <sub>2</sub> )	C <sub>44</sub> H <sub>26</sub> O <sub>8</sub> ·2(C <sub>6</sub> H <sub>4</sub> Cl <sub>2</sub> )	C <sub>44</sub> H <sub>26</sub> O <sub>8</sub>
Fw	1270.61	976.63	682.65
Crystal system	monoclinic	monoclinic	triclinic
Space group	<i>P</i> 2 <sub>1</sub> / <i>c</i>	<i>P</i> 2 <sub>1</sub> / <i>c</i>	<i>P</i> -1
<i>a</i> / Å	7.3723(2)	7.5511(4)	7.5864(17)
<i>b</i> / Å	15.6634(4)	11.4435(8)	9.404(3)
<i>c</i> / Å	25.1288(6)	26.3091(16)	13.016(3)
$\alpha$ / °	90	90	78.06 (2)
$\beta$ / °	94.144(2)	92.902(5)	86.453 (17)
$\gamma$ / °	90	90	67.84 (2)
<i>V</i> / Å <sup>3</sup>	2894.17(13)	2270.5(2)	841.3 (4)
<i>d</i> / g·cm <sup>-3</sup>	1.458	1.429	1.348
T / K	113	113	100
Crystal size / mm	0.49 × 0.15 × 0.058	0.13 × 0.07 × 0.03	0.10 × 0.08 × 0.02
No. of measured reflections	35154	21812	8327
No. of independent reflections	7651	5753	3644
<i>R</i> <sub>1</sub> ( <i>I</i> > 2σ( <i>I</i> ))	0.0568	0.0720	0.2112
<i>wR</i> <sub>2</sub> (all)	0.1237	0.1916	0.597
GOF	1.022	1.036	2.114
CCDC Nos.	2206159	2255738	2255739
Ref.	Ref. S7	This work	This work

**Table S1.** Continued.

	<b>CP-Py-1(TCB)</b>	<b>CP-Py-2(TCB)</b>
Formular	C <sub>44</sub> H <sub>26</sub> O <sub>8</sub>	C <sub>44</sub> H <sub>26</sub> O <sub>8</sub> ·2(C <sub>6</sub> H <sub>3</sub> Cl <sub>3</sub> )
Fw	682.65	1045.51
Crystal system	monoclinic	monoclinic
Space group	P2 <sub>1</sub> /c	C2/m
<i>a</i> / Å	6.7428(3)	27.5399(14)
<i>b</i> / Å	15.8023(9)	11.8206(8)
<i>c</i> / Å	27.6306(12)	7.2355(4)
α / °	90	90
β / °	93.044(4)	92.898(5)
γ / °	90	90
<i>V</i> / Å <sup>3</sup>	2939.9(2)	2352.4(2)
<i>d</i> / g·cm <sup>-3</sup>	0.771	1.476
T / K	113	113
Crystal size / mm	0.29 × 0.16 × 0.07	0.18 × 0.10 × 0.04
No. of measured reflections	30394	17520
No. of independent reflections	7603	3735
<i>R</i> <sub>1</sub> ( <i>I</i> > 2σ( <i>I</i> ))	0.0957	0.0609
w <i>R</i> <sub>2</sub> (all)	0.3294	0.1434
GOF	1.044	1.047
CCDC Nos.	2255740	2255741
Ref.	This work	This work

**Table S1.** Continued.

	<b>CP-Py-1(DMAri)</b>	<b>CP-Py-2(DMAri)</b>	<b>CP-Py-1(MeNaph)</b>
Formular	C <sub>44</sub> H <sub>26</sub> O <sub>8</sub>	C <sub>44</sub> H <sub>26</sub> O <sub>8</sub> ·3(C <sub>8</sub> H <sub>11</sub> N)	C <sub>44</sub> H <sub>26</sub> O <sub>8</sub> ·3(C <sub>11</sub> H <sub>10</sub> )
Fw	682.65	1046.18	1109.21
Crystal system	monoclinic	monoclinic	monoclinic
Space group	<i>C2/m</i>	<i>P2<sub>1</sub>/c</i>	<i>P2<sub>1</sub>/c</i>
<i>a</i> / Å	23.4820(13)	7.4693 (4)	7.6554(13)
<i>b</i> / Å	17.2143(10)	14.233 (2)	15.342(3)
<i>c</i> / Å	7.5294(3)	24.1720 (16)	24.524(5)
$\alpha$ / °	90	90	90
$\beta$ / °	94.013(5)	94.080 (6)	94.763(18)
$\gamma$ / °	90	90	90
<i>V</i> / Å <sup>3</sup>	3036.1(3)	2563.2 (4)	2870.4(10)
<i>d</i> / g·cm <sup>-3</sup>	0.747	1.356	1.283
T / K	100	100	113
Crystal size / mm	0.20 × 0.09 × 0.04	0.12 × 0.09 × 0.03	0.08 × 0.07 × 0.01
No. of measured reflections	18358	32342	43799
No. of independent reflections	3692	6267	7579
<i>R</i> <sub>1</sub> ( <i>I</i> > 2σ( <i>I</i> ))	0.0911	0.1210	0.1408
<i>wR</i> <sub>2</sub> (all)	0.3094	0.4120	0.3606
GOF	1.232	1.255	1.020
CCDC Nos.	2255742	2255743	2262072
Ref.	This work	This work	This work

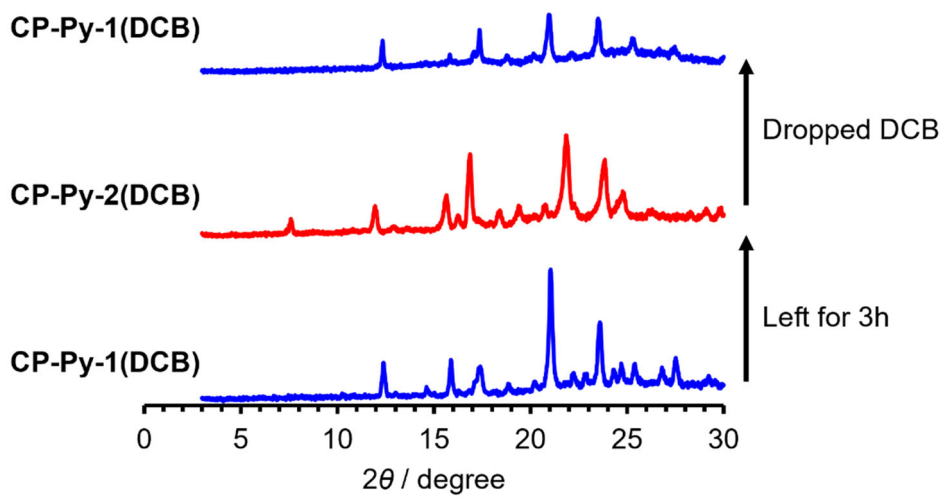


**Fig. S1** PXRD pattern of **CP-Py-2(DCB)** after added DCB.

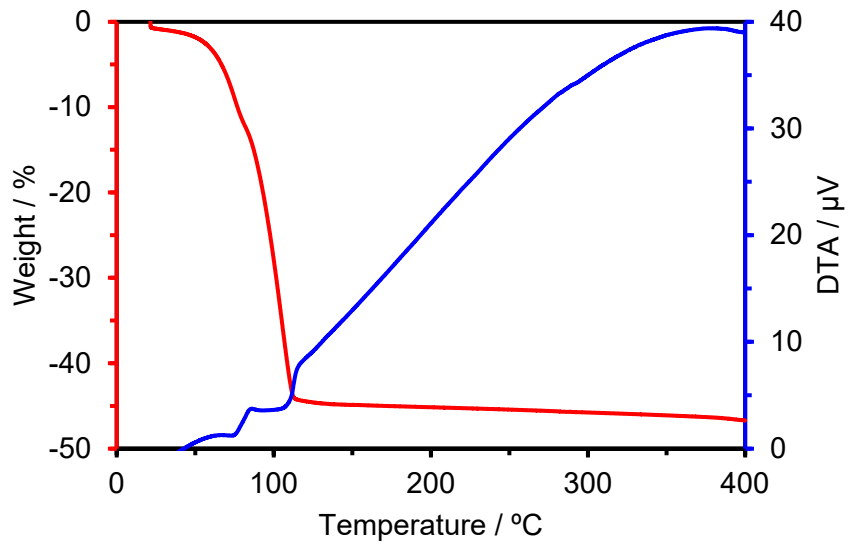


**Fig. S2** TGA-DTA curves of **CP-Py-1(DCB)**.

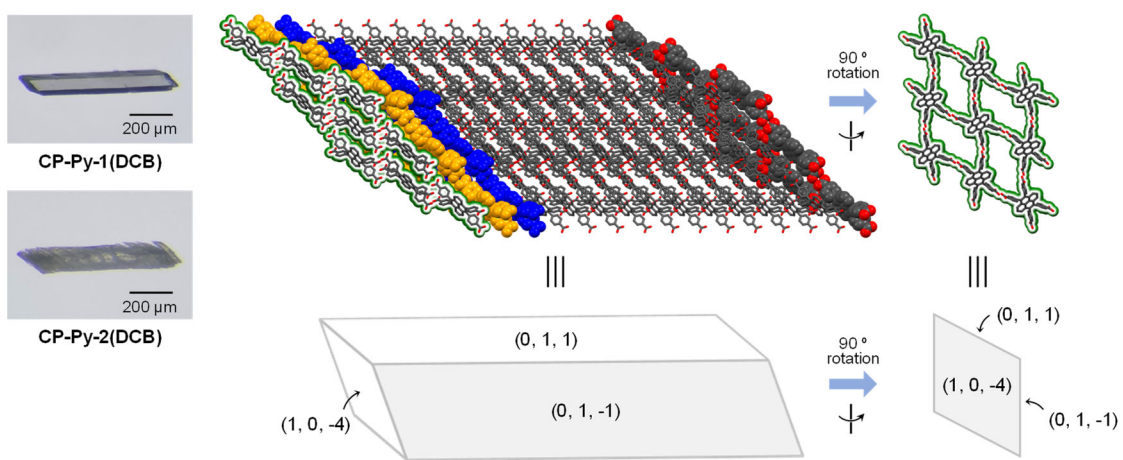


**Fig. S3** Morphology of a single crystal and the corresponding molecular arrangements of **CP-Py-1(DCB)**.

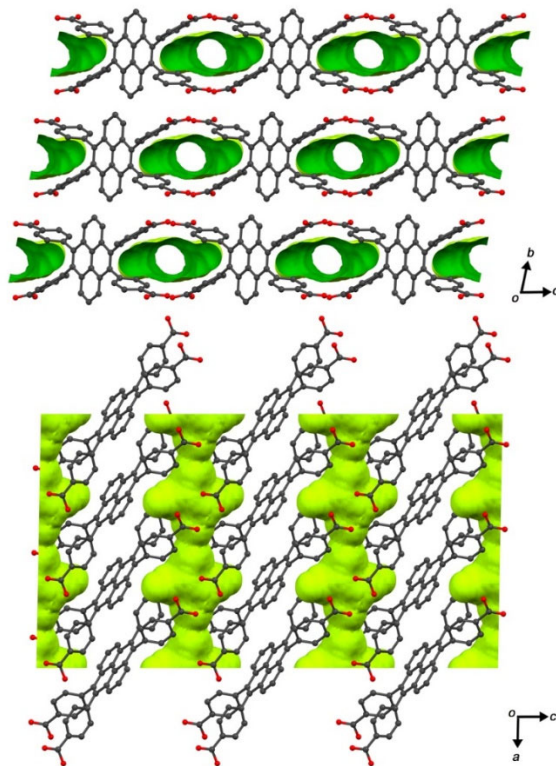


**Fig. S4** Visualized void surface of **CP-Py-3**. Projection from the *a* axis (top) and the *b* axis (bottom). The surface was generated by Mercury software with probe radius of 1.2 Å and grid spacing of 0.2 Å.

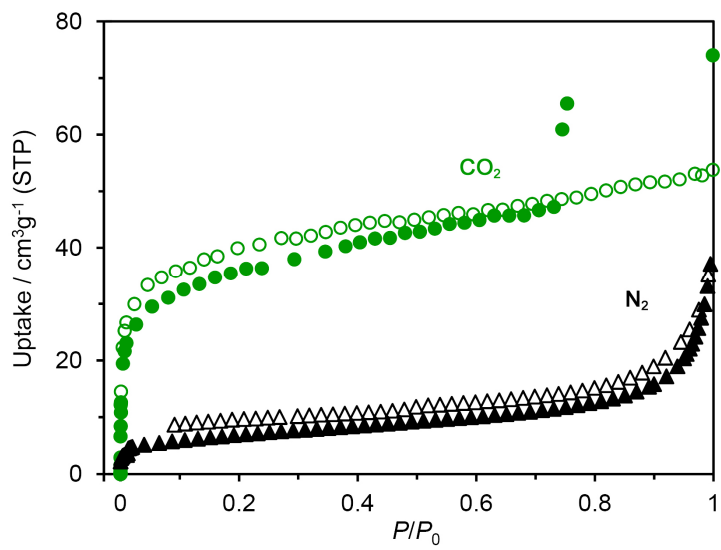


**Fig. S5**  $\text{CO}_2$  (green circle) and  $\text{N}_2$  (black triangle) sorption isotherms of **CP-Py-3** recorded at 195 K and 77 K, respectively. Solid and open symbols correspond to adsorption and desorption processes, respectively.

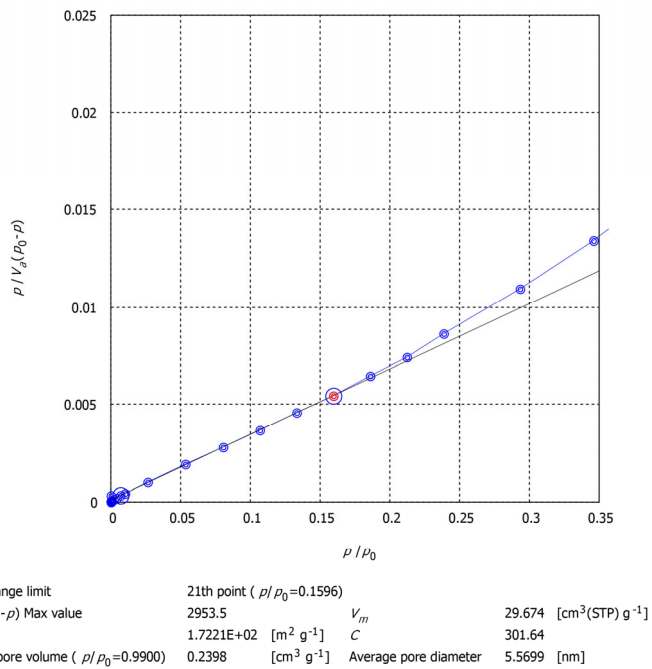


**Fig. S6** BET plot of CP-Py-3 based on CO<sub>2</sub> adsorption isotherm.

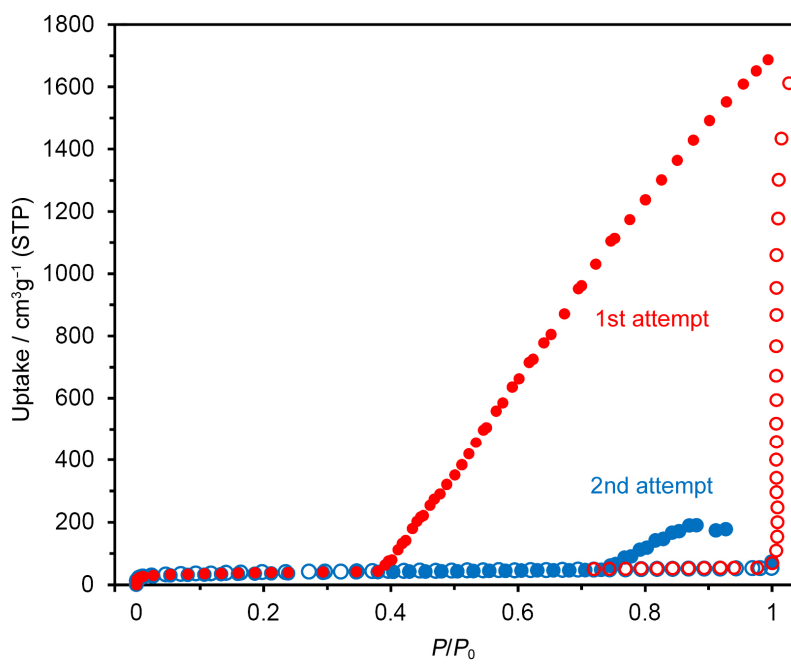


**Fig. S7** Anomalous absorption behavior of CP-Py-3 in CO<sub>2</sub> adsorption experiments.

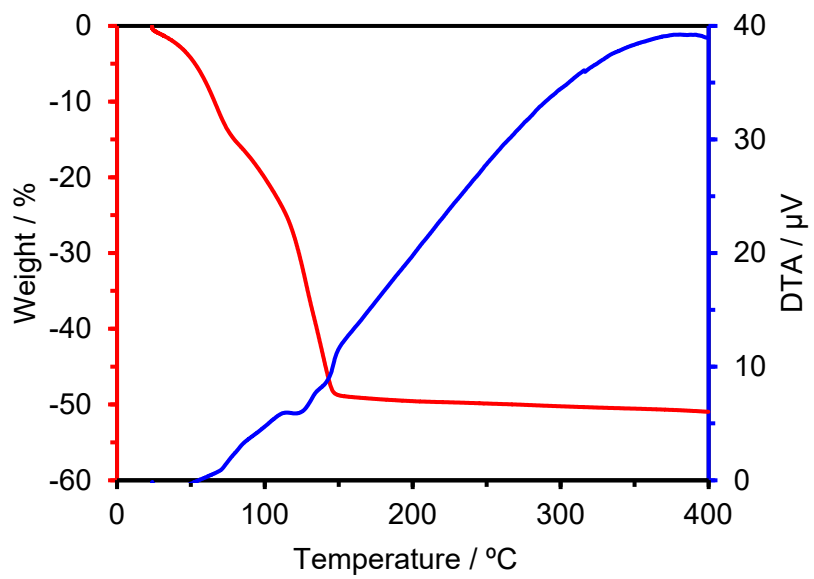


**Fig. S8** TGA-DTA curves of **CP-Py-1(TCB)**.

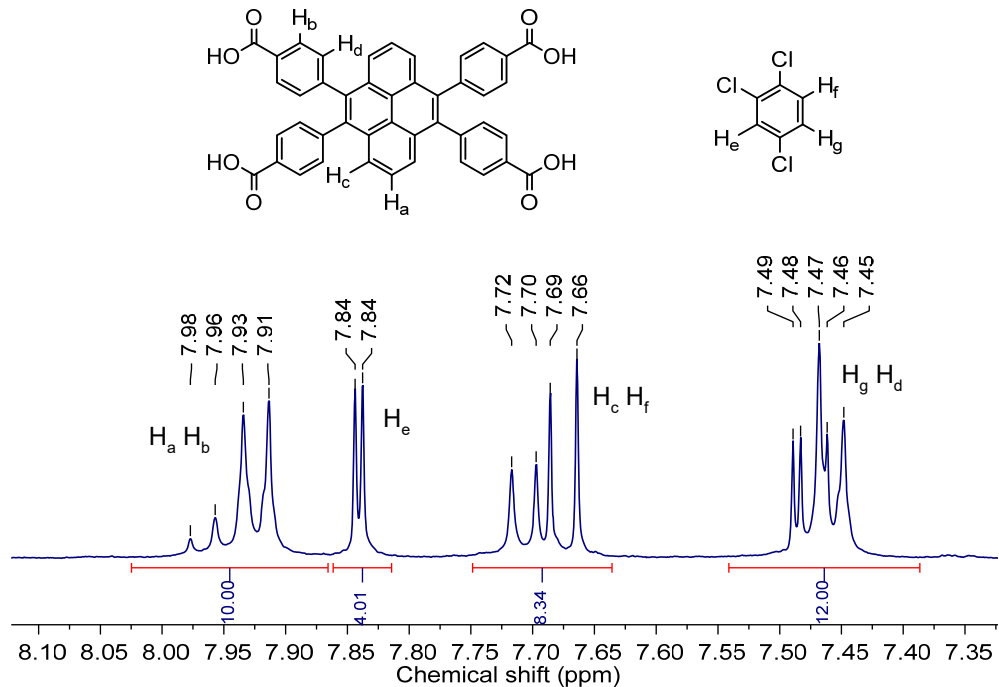


**Fig. S9** <sup>1</sup>H NMR (400 MHz) spectrum of **CP-Py-1(TCB)** dissolved in DMSO-*d*<sub>6</sub>.

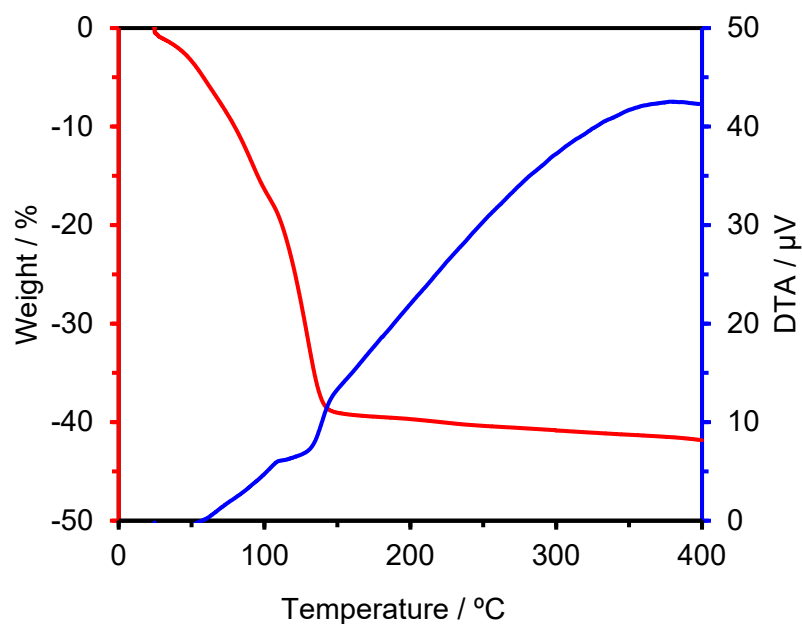


**Fig. S10** TGA-DTA curves of **CP-Py-1(DMAri)**.

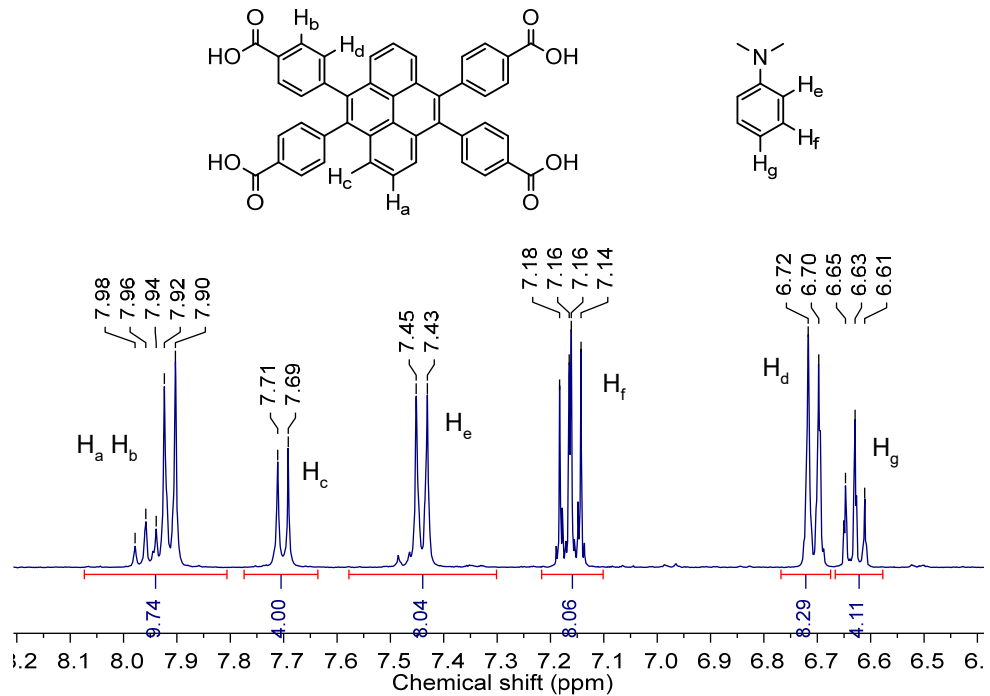


**Fig. S11** <sup>1</sup>H NMR (400 MHz) spectrum of **CP-Py-1(DMAri)** dissolved in DMSO-*d*<sub>6</sub>.

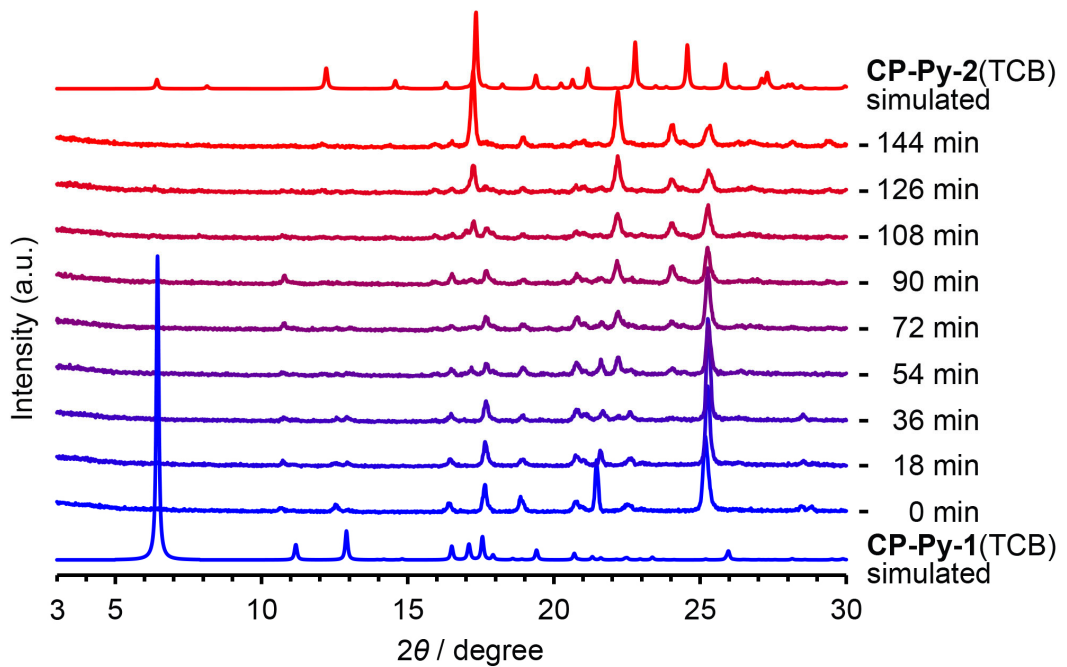


**Fig. S12.** PXRD pattern changes from **CP-Py-1(TCB)** to **CP-Py-2(TCB)**.

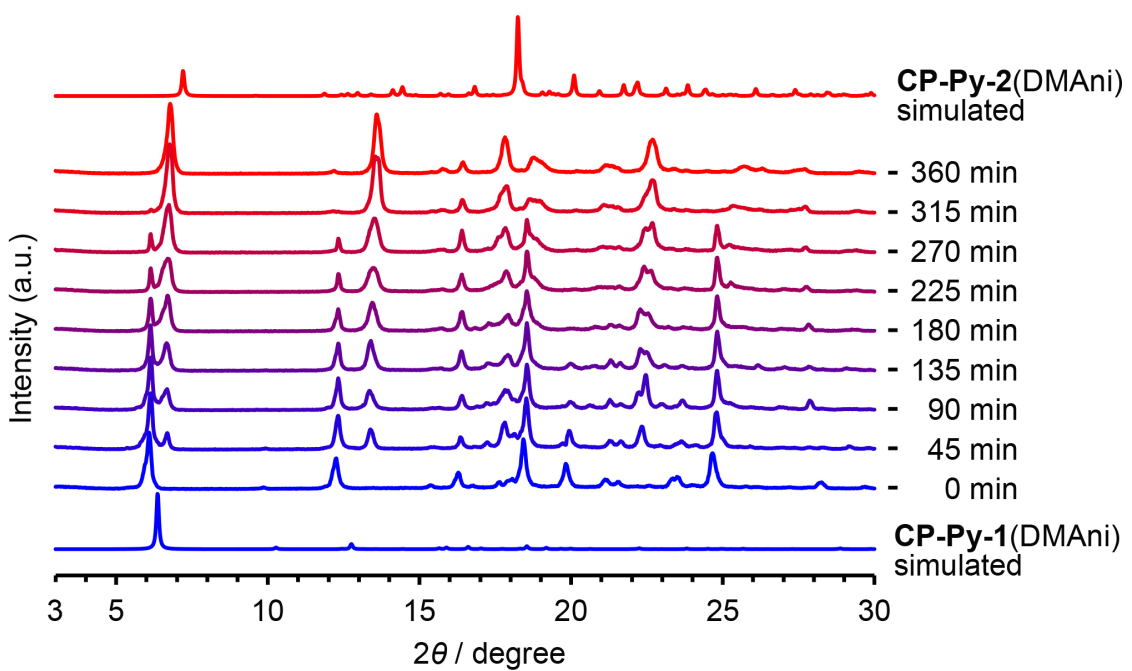


**Fig. S13.** PXRD pattern changes from **CP-Py-1(DMAni)** to **CP-Py-2(DMAni)**.

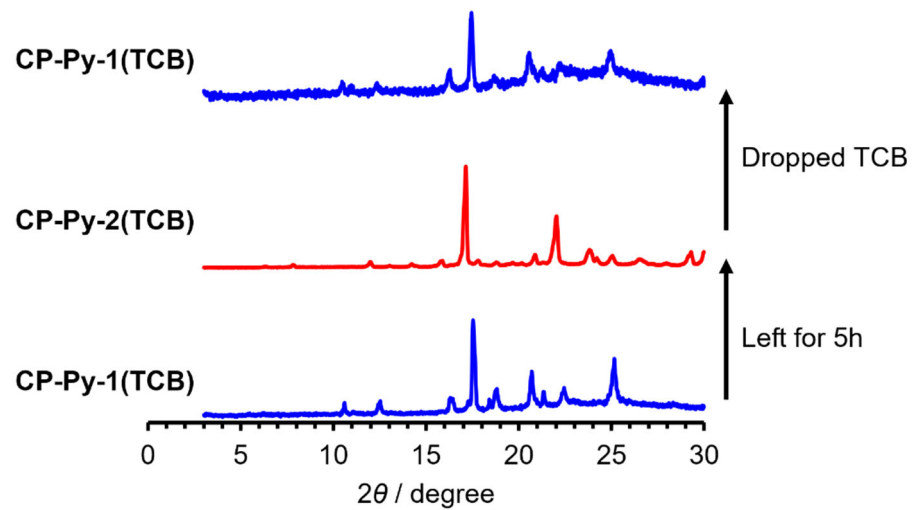


**Fig. S14** PXRD pattern of CP-Py-2(TCB) after added TCB.

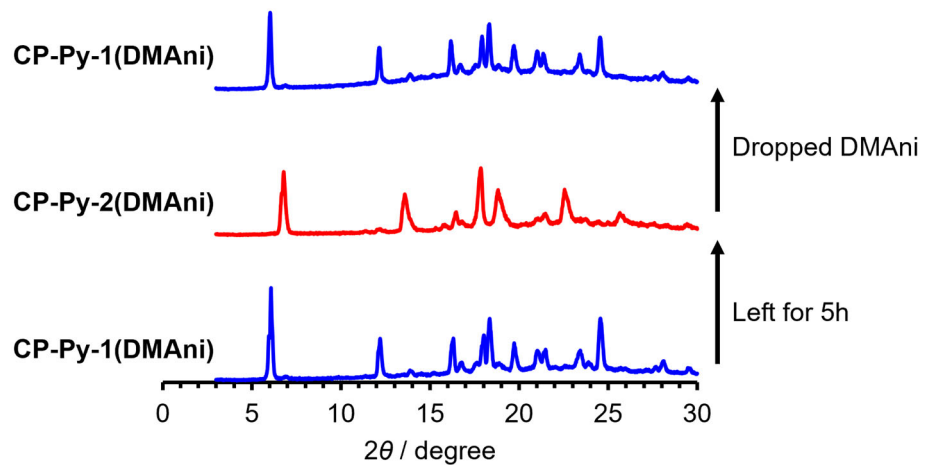


**Fig. S15** PXRD pattern of CP-Py-2(DMAni) after added DMAni.

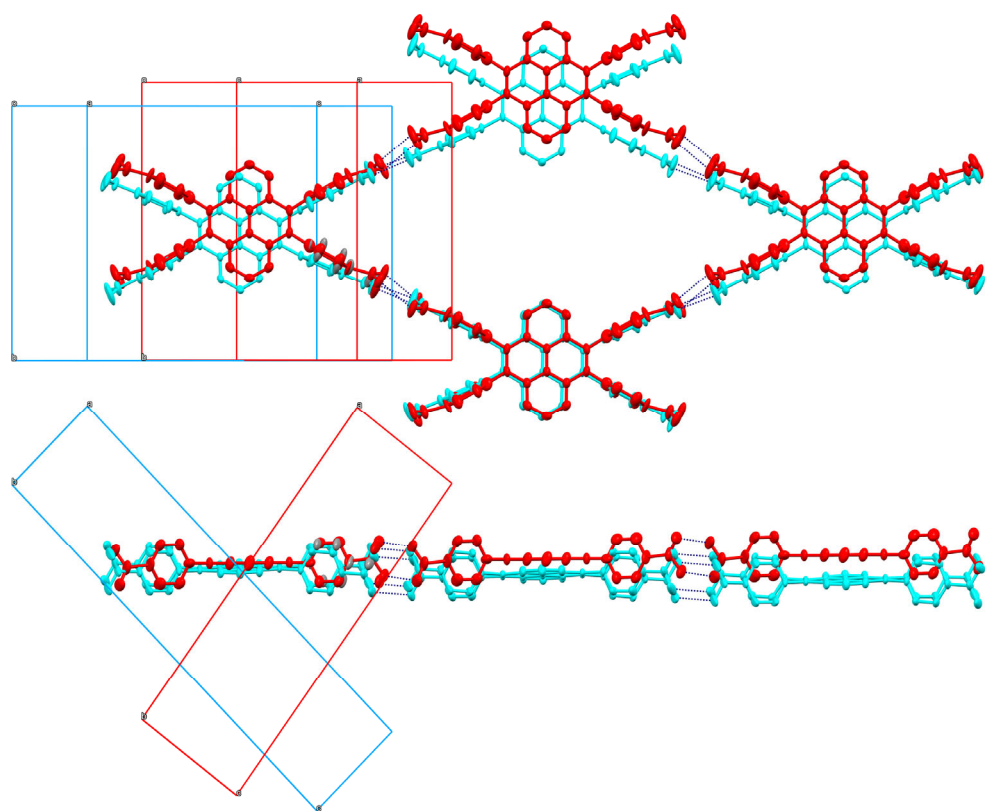


**Fig. S16** Structural similarity of **CP-Py-1(TCB)** (cyan) and **CP-Py-1(DMAri)** (red). The framework shown in top corresponds to one layer allowed in the side view at the bottom.

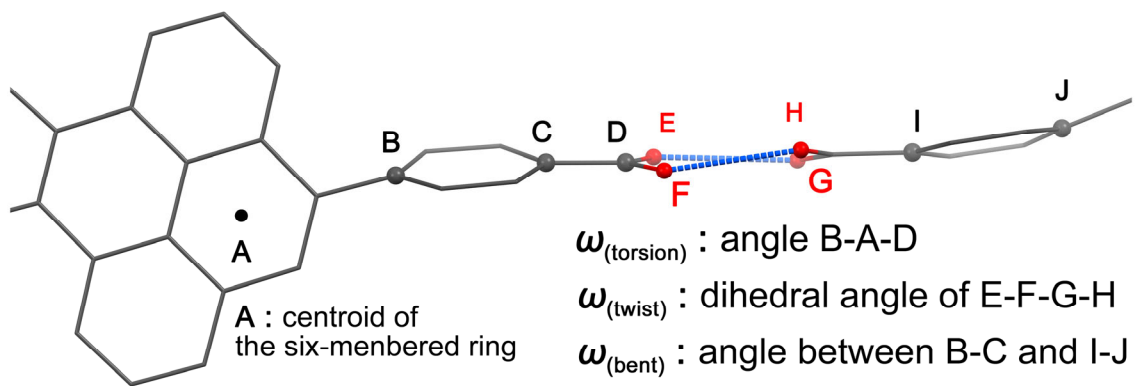


**Fig. S17** Definition of the structural parameters:  $\omega_{(\text{torsion})}$ ,  $\omega_{(\text{twist})}$ , and  $\omega_{(\text{bent})}$ , which characterize versatile shapes of the framework.

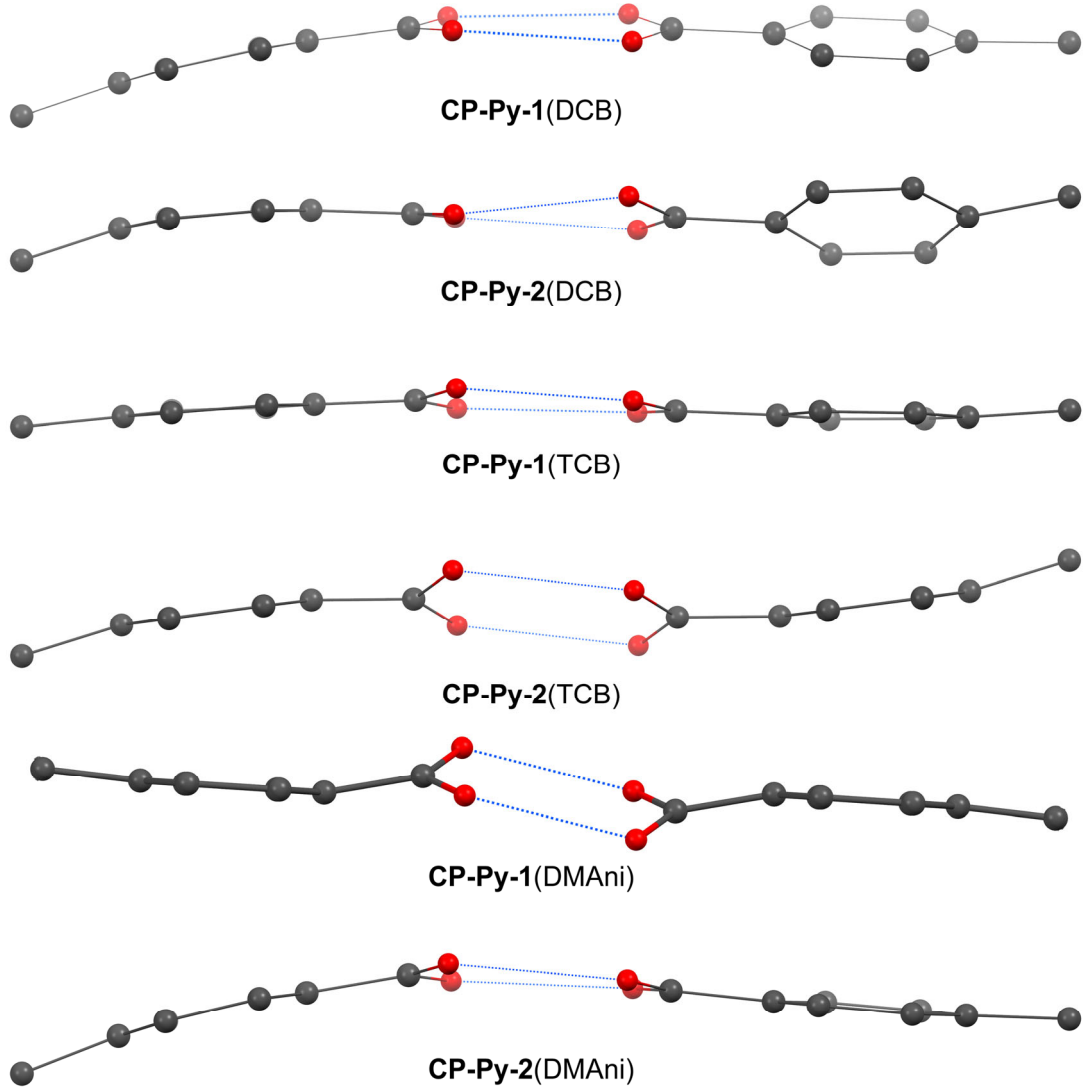


**Fig. S18** Selected side views of the H-bonded dimer moieties of **CP-Py-1(DCB)**, **CP-Py-2(DCB)**, **CP-Py-1(TCB)**, **CP-Py-2(TCB)**, **CP-Py-1(DMANi)**, and **CP-Py-2(DMANi)**.

### 3. References

- S1. C. F. MacRae, I. Sovago, S. J. Cottrell, P. T. A. Galek, P. McCabe, E. Pidcock, M. Platings, G. P. Shields, J. S. Stevens, M. Towler and P. A. Wood, *J. Appl. Crystallogr.*, 2020, **53**, 226.
- S2. Rigaku Oxford Diffraction (2015), Software CrysAlisPro 1.171.38.41o. Rigaku Corporation, Tokyo, Japan.
- S3. G. M. Sheldrick, *Acta Crystallogr. Sect. A*, 2015, **71**, 3.
- S4. (a) Rigaku (2018). CrystalStructure. Version 4.3. Rigaku Corporation, Tokyo, Japan. (b) O. V. Dolomanov, L. J. Bourhis, R. J. Gildea, J. A. K. Howard and H. Puschmann, *H. J. Appl. Cryst.*, 2009, **42**, 339. (c) L. J. Bourhis, O. V. Dolomanov, R. J. Gildea, J. A. K. Howard and H. Puschmann, *Acta Crystallogr. Sect. A*, 2015, **71**, 59.
- S5. G. M. Sheldrick, *Acta Crystallogr. Sect. C*, 2015, **71**, 3.
- S6. (a) P. v. d. Sluis and A. L. Spek, *Acta Crystallogr. Sect. A*, 1990, **46**, 194. (b) A. L. Spek, *Acta Crystallogr. Sect. D*, 2009, **65**, 148.
- S7. T. Hashimoto, R. Oketani, M. Nobuoka, S. Seki and I. Hisaki, *Angew. Chem. Int. Ed.*, 2023, **62**, e202215836.